

Non-zero transverse single spin asymmetry of very forward π^0 in polarized $p + p$ collisions at $\sqrt{s} = 510$ GeV

M. H. Kim^{*1,2} for the RHICf Collaboration

1 RIKEN BNL Research Center, Brookhaven National Laboratory, Upton, New York
11973-5000, USA

2 Korea University, Seoul 02841, Korea

* jipangie@korea.ac.kr

March 20, 2022

1 Abstract

2 The RHICf experiment measured transverse single spin asymmetry of very
3 forward ($\eta > 6$) π^0 from polarized $p + p$ collisions at $\sqrt{s} = 510$ GeV. In order to
4 measure it precisely, we installed a new electromagnetic calorimeter at zero-
5 degree area of the STAR experiment at the Relativistic Heavy Ion Collider
6 (RHIC) and measured the π^0 s over the kinematic range of $x_F > 0.25$ and
7 $0 < p_T < 1$ GeV/ c in June 2017. A clear non-zero asymmetry was observed
8 even in low $p_T < 1$ GeV/ c showing a similar x_F dependence with that of the
9 forward ($2 < \eta < 4$) π^0 . A possible diffractive contribution may need to be
10 taken into account to explain the very forward π^0 asymmetry. RHICf-STAR
11 combined analysis and follow-up experiment will give a clue to understand it
12 qualitatively.

13

14 Contents

15	1 Introduction	1
16	2 RHICf Experiment	2
17	3 Data analysis	3
18	4 Results	4
19	5 Conclusion	6
20	6 Future Prospect	6
21	References	7

22

23

24 1 Introduction

25 Transverse single spin asymmetry (A_N) is a powerful observable for understanding the
26 spin-involved production mechanism in the polarized $p + p$ collision. It is defined by a

27 left-right cross section asymmetry,

$$A_N = \frac{\sigma_L - \sigma_R}{\sigma_L + \sigma_R}, \quad (1)$$

28 where the $\sigma_{L(R)}$ is the cross section of a particle produced in the left (right) side with
29 respect to the beam polarization.

30 Large non-zero asymmetries in the π^0 production have been discussed only in the
31 quarks and gluons' degrees of freedom. It has been measured in a wide range of collision
32 energies [1–5] and these results have been explained by transverse momentum dependent
33 (TMD) [6–8] and higher twist functions [9–11] in an initial or final state with the transverse
34 motions of quarks and gluons.

35 Recently, further analysis results [12–14] showed a strange behavior in the forward π^0
36 asymmetry. Bigger asymmetry was observed in more isolated π^0 event which is connected
37 to the diffractive process. In this analysis, the π^0 was considered as isolated one when its
38 energy fraction to the detected electromagnetic particles was close to 1. In this case, since
39 the π^0 carries larger energy fraction, the asymmetry nature could be biased. However, it
40 also gives us a possibility of the diffractive contribution to the π^0 asymmetry because it is
41 also expected that there is few particles around it when it is produced by the diffractive
42 process, thereby the π^0 asymmetry induced by the diffractive process may be observed in
43 this analysis. This means the non-zero asymmetry could be correlated with not only the
44 partonic interaction but also the diffractive one.

45 In order to study the diffractive contribution to the π^0 asymmetry, the RHICf exper-
46 iment measured the A_N in the very forward π^0 production. The diffractive process is
47 expected to dominate when the produced particle is measured in the very forward region.

48 2 RHICf Experiment

49 We installed an electromagnetic calorimeter (RHICf detector) which had been originally
developed for the LHCf experiment [15] in front of a STAR hadronic calorimeter, zero-

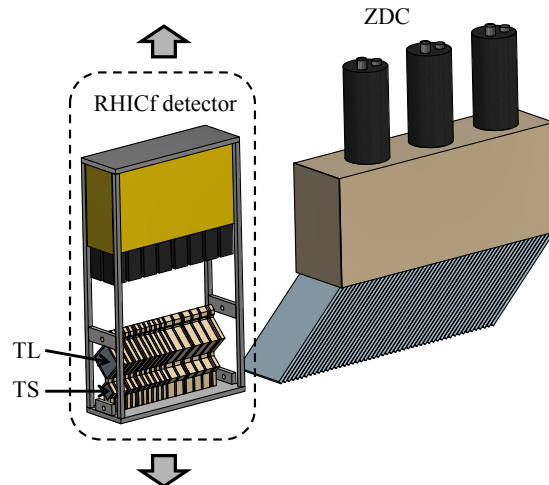


Figure 1: Schematic drawing of the RHICf detector installed in front of the ZDC. We moved the detector vertically to cover p_T from 0.0 to 1.0 GeV/ c .

50
51 degree calorimeter (ZDC) [16], which was located 18 m away from the beam interaction
52 point and took the data in June 2017. Figure 1 shows the schematic drawing of the
53 experimental setup.

54 The RHICf detector consists of two sampling calorimeters, the large (TL, 40 mm
 55 dimension) and small (TS, 20 mm dimension) towers. Both towers are composed of 17
 56 layers of tungsten absorber with a 44 radiation lengths in total, 16 layers of GSO plate
 57 for energy measurement, and 4 layers of GSO bars. Particle energy is reconstructed by
 58 the energy deposits of the GSO plates. Position is reconstructed by the GSO bar layers,
 59 which are covered by X-Y pairs of GSO bars with 1 mm dimension.

60 We measured the very forward π^0 from the polarized $p+p$ collisions at $\sqrt{s} = 510$ GeV.
 61 In order to measure the wide p_T coverage, we used the radial polarization which was the
 62 90° -rotated one than usual vertical polarization. We also moved the detector vertically
 63 so that the zero-degree direction of the beam faced the center of the TL, the center of
 64 the TS, and 24 mm below the center of the TS. We requested larger β^* value of 8 m and
 65 lower luminosity $\sim 10^{31}$ cm $^{-2}$ s $^{-1}$ than usual to make the systematic uncertainty by the
 66 angular beam divergence small. The β^* is an indicator for how much the beam is squeezed.
 67 With these detector positions and special settings, π^0 s over the longitudinal momentum
 68 fraction range of $x_F > 0.25$ and the transverse momentum range of $0 < p_T < 1$ GeV/ c
 69 were measured. For the measured π^0 s, the RHICf detector has an energy resolution of
 70 $2.5\% \sim 3.5\%$ and p_T resolution of $3.0\% \sim 4.5\%$.

71 π^0 s could be identified by measuring two decayed photons in each tower (Type-I) or
 72 both ones in same tower (Type-II). A Type-I π^0 trigger was used for the measurement of the
 73 Type-I events. It was operated when the energy deposits of three successive layers of both
 74 towers are larger than 45 MeV. Since the electromagnetic shower stops the development
 75 in the middle of the detector, only the upstream seven layers were used for this trigger.
 76 The Type-II events were measured by a high electromagnetic (high-EM) trigger. It was
 77 operated when the energy deposit of the fourth layer of either tower is larger than 500
 78 MeV.

79 3 Data analysis

80 Due to the detector geometry, we used following luminosity formula to calculate the π^0
 81 asymmetry

$$A_N = \frac{1}{PD_\phi} \left(\frac{N_L - RN_R}{N_L + RN_R} \right), \quad (2)$$

82 where P is the beam polarization, $N_{L(R)}$ is the number of detected π^0 s in the left (right)
 83 side of the beam polarization. R is the luminosity ratio of the spin directions resulting into
 84 the events to right and left sides. It was estimated using STAR beam beam counter (BBC)
 85 [17] and vertex position detector (VPD) [18]. D_ϕ is a correction factor to compensate the
 86 diluted asymmetry by the azimuthal angle distribution of the detected π^0 s. Only the
 87 Type-I π^0 triggered events were used for the asymmetry calculation of the Type-I events
 88 and high-EM triggered events for the Type-II events to be free from the effect of the
 89 different detection efficiencies.

90 π^0 s to be analyzed were identified using invariant mass distribution of two detected
 91 photons. Figure 2 shows the reconstructed invariant mass distribution. In this distribu-
 92 tion, a clear π^0 peak (blue dashed line) was observed in the widely smeared background
 93 events (black filled histogram). The background mostly comes from two accidental pho-
 94 tons from different π^0 s. Superposition of the Gaussian (for describing the π^0 events) and
 95 the 6th order of polynomial (for describing the background events) function was used to
 96 fit the invariant mass distribution. 3σ width of the Gaussian peak was considered as the
 97 final π^0 candidate. The effect of the background events included in the final π^0 sample

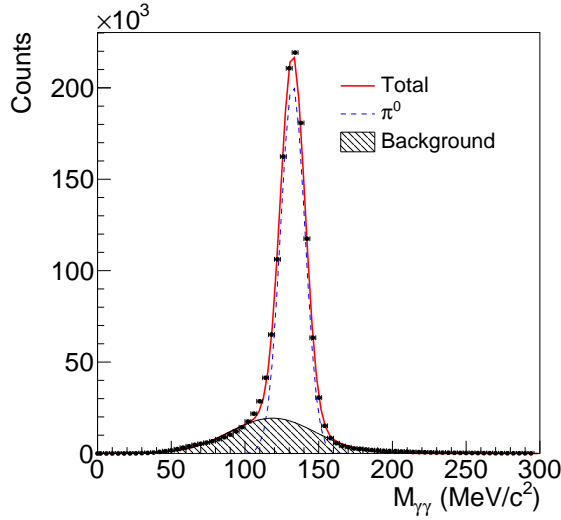


Figure 2: Reconstructed two photon invariant mass distribution of Type-I event in $x_F > 0.25$ and $0.0 < p_T < 1.0$ GeV/ c .

98 was subtracted using the following equation

$$A_N^S = \left(1 + \frac{N_B}{N_S}\right) A_N^{S+B} - \left(\frac{N_B}{N_S}\right) A_N^B, \quad (3)$$

99 where A_N^{S+B} , A_N^S , and A_N^B are the estimated asymmetries in the signal+background, signal
 100 only and background only regions. The A_N^B was estimated using the events whose invariant
 101 mass was further than 5σ of the Gaussian peak and the signal to background ratio, $\frac{N_B}{N_S}$,
 102 was calculated from the fit result.

103 The π^0 asymmetry was calculated as functions of x_F and p_T to study their correla-
 104 tion. Systematic uncertainties by the polarization and beam center estimations, and the
 105 background subtraction were included. The effect of the smearing due to the finite x_F and
 106 p_T resolutions were studied by GEANT4 using the single π^0 beam which was artificially
 107 weighted to reproduce the asymmetry, but they were negligible. For each bin divided by
 108 selected x_F and p_T values, more than 90% of migrated events were from $\delta x_F < 0.025$ and
 109 $\delta p_T < 0.035$ GeV/ c of the bin boundaries. The differences between the calculated and
 110 true $\langle x_F \rangle$, $\langle p_T \rangle$, A_N values of each bin were less than 0,008, 0.009 GeV/ c , and 0.0015,
 111 respectively.

112 To find any missing systematic uncertainties, a “bunch shuffling” analysis was pro-
 113 ceeded. It is done by randomizing the spin patterns and reconstructing the A_N again.
 114 Since the spin patterns are randomized, ideally, the reconstructed A_N should be fluctu-
 115 ated around 0 with its statistical uncertainty if there is no systematic source missed. The
 116 bunch shuffled asymmetries were consistent with zero in the comparable fluctuation with
 117 the statistical uncertainties. We conclude that there are no noticeable false asymmetries
 118 in this analysis.

119 4 Results

120 Figure 3 shows the A_N of very forward π^0 as functions of x_F and p_T . Increasing A_N as a
 121 function of p_T up to ~ 0.2 is clearly shown in Figure 3 (a) and the corresponding p_T range

122 is where the diffractive process dominates. In Figure 3 (b), the backward asymmetries
 123 which are the ones in the opposite side of the polarized beam are consistent with zero.
 124 The forward asymmetry is also consistent with zero at very low $p_T < 0.07$ GeV/ c , but it
 starts to increase as a function of x_F as p_T increases.

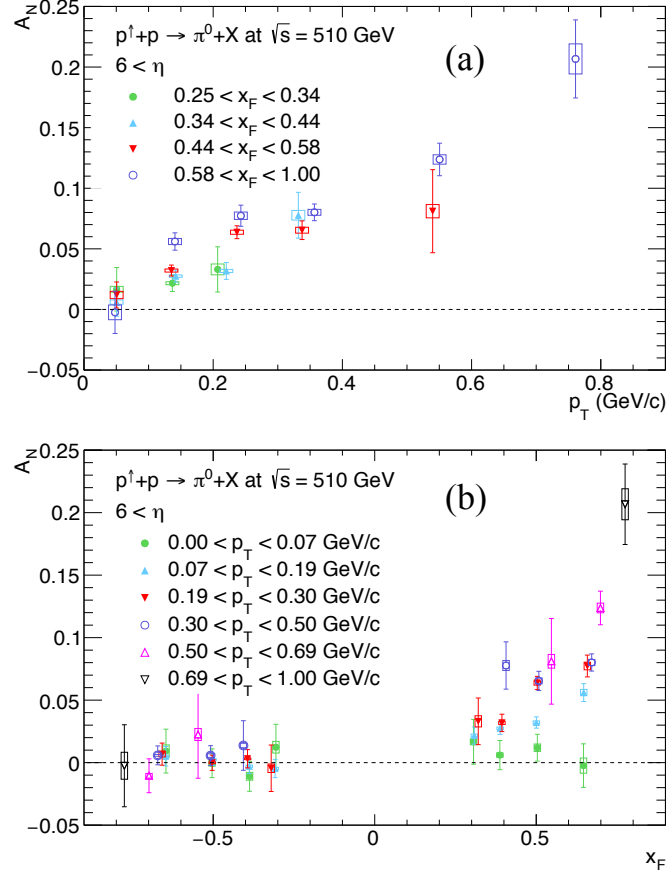


Figure 3: A_N of the very forward π^0 s as functions of (a) p_T for several x_F ranges and (b) x_F for several p_T ranges. Only forward A_N was presented in (a). Error bars represent the statistical uncertainties, and the boxes represent the systematic uncertainties.

125

126

127

128

129

130

131

132

133

134

135

136

Figure 4 shows the comparison of the RHICf data with the forward π^0 asymmetries previously measured by FNAL, PHENIX, and STAR. It shows that the increasing asymmetries of the very forward π^0 get comparable with the forward π^0 ones at higher p_T though it is still smaller than 1 GeV/ c . The RHICf result also shows the same x_F scaling with the forward π^0 ones. The diffractive process may contribute to the asymmetries at higher p_T than it has been expected. Since the RHICf data may be also a tail of the partonic one, more detailed analysis than inclusive one is necessary. Correlations with STAR's central detectors and Roman pots will make it possible by identifying from which process the π^0 with non-zero asymmetry comes. It is also desirable to investigate the same observables in the unexplored kinematic region between 0.8~2.0 GeV/ c where the fractions of both partonic and diffractive processes are comparable.

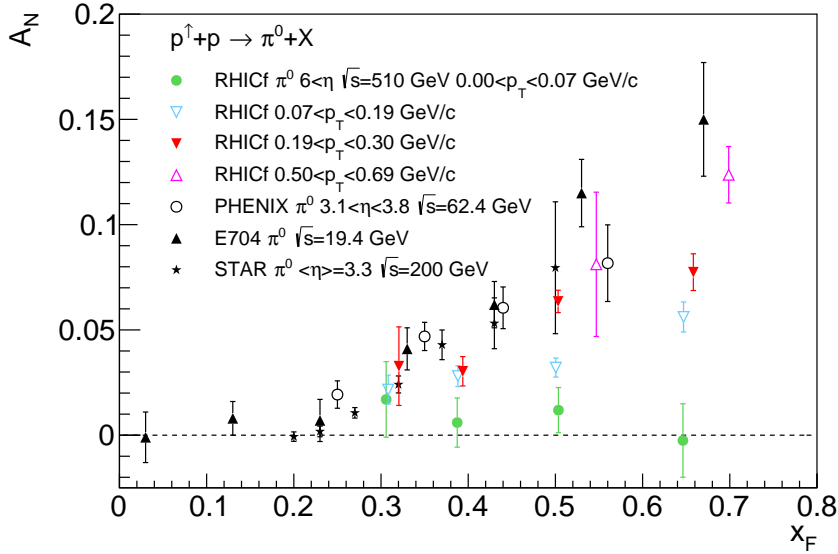


Figure 4: Comparison of the RHCf data with the previously measured A_N of the forward π^0 s as a function of x_F .

137 5 Conclusion

138 The role of the diffractive process to the π^0 asymmetry can be studied by measuring the
 139 A_N of the very forward π^0 . At low $p_T < 1$ GeV/c where the diffractive process is expected
 140 to dominate, large non-zero asymmetries increasing as functions of both x_F and p_T have
 141 been observed for the first time from the polarized $p + p$ collisions at $\sqrt{s} = 510$ GeV.
 142 The asymmetries show an approximate x_F scaling with the forward π^0 ones, which may
 143 indicate a possible diffractive contribution to the π^0 asymmetries. The RHCf result will
 144 be further investigated by RHCf-STAR combined analysis and a follow-up experiment,
 145 RHCf-II.

146 6 Future Prospect

147 In order to more deeply understand the RHCf result, RHCf-STAR combined analysis has
 148 been started. Using STAR detectors covering each η region, the type of the production
 149 mechanism is expected to be identified.

150 A follow-up experiment (RHCf-II) is also being prepared. To measure more various
 151 particles and for higher statistics, a larger detector of 8 cm \times 18 cm dimension is planned to
 152 be constructed. Technology of ALICE FoCal-E [19] will be transferred to the construction
 153 of the RHCf-II detector. Currently, we're optimizing the definite design of the detector
 154 and planning to take the data in 2024 at STAR.

155 **Funding information** This program is partly supported by the U.S.-Japan Science
 156 and Technology Cooperation Program in High Energy Physics, JSPS KAKENHI (No.
 157 JP26247037 and No. JP18H01227), the joint research program of the Institute for Cosmic
 158 Ray Research (ICRR), University of Tokyo, and the National Research Foundation of
 159 Korea (No. 2016R1A2B2008505 and No. 2018R1A5A1025563), and "UNICT 2020-22

160 Linea 2” program, University of Catania.

161 References

- 162 [1] A. Adare *et al.* (PHENIX Collaboration), *Measurement of transverse-single-spin*
163 *asymmetries for midrapidity and forward-rapidity production of hadrons in polar-*
164 *ized p+p collisions at $\sqrt{s} = 200$ and 62.4 GeV*, Phys. Rev. D **90**, 012006 (2014),
165 doi:10.1103/PhysRevLett.101.222001.
- 166 [2] B. I. Abelev *et al.* (STAR Collaboration), *Forward Neutral Pion Transverse Single*
167 *Spin Asymmetries in p+p Collisions at $\sqrt{s} = 200$ GeV*, Phys. Rev. Lett. **101**, 222001
168 (2008), doi:10.1103/PhysRevLett.101.222001.
- 169 [3] D. L. Adams *et al.* (E581 and E704 Collaborations), *Comparison of spin asymmetries*
170 *and cross-sections in π^0 production by 200-GeV polarized anti-protons and protons*,
171 Phys. Lett. B **261**, 201 (1991), doi:10.1016/0370-2693(91)91351-U.
- 172 [4] B. E. Bonner *et al.*, *Analyzing Power Measurement in Inclusive π^0 Production at*
173 *High x_F* , Phys. Rev. Lett. **61**, 1918 (1988), doi:10.1103/PhysRevLett.61.1918.
- 174 [5] R. D. Klem *et al.*, *Measurement of Asymmetries of Inclusive Pion Production in*
175 *Proton Proton Interactions at 6-GeV/c and 11.8-GeV/c*, Phys. Rev. Lett. **36**, 929
176 (1976), doi:10.1103/PhysRevLett.36.929.
- 177 [6] D. W. Sivers, *Single Spin Production Asymmetries from the Hard Scattering of Point-*
178 *Like Constituents*, Phys. Rev. D **41**, 83 (1990). doi:10.1103/PhysRevD.41.83.
- 179 [7] J. C. Collins, *Fragmentation of transversely polarized quarks probed in trans-*
180 *verse momentum distributions*, Nucl. Phys. B **396**, 161 (1993), doi:10.1016/0550-
181 3213(93)90262-N.
- 182 [8] J. C. Collins, S. F. Heppelmann, and G. A. Ladinsky, *Measuring transversity densities*
183 *in singly polarized hadron-hadron and lepton-hadron collisions* Nucl. Phys. B **420**, 565
184 (1994), doi:10.1016/0550-3213(94)90078-7.
- 185 [9] J. W. Qiu and G. F. Sterman, *Single transverse spin asymmetries in direct photon*
186 *production*, Nucl. Phys. B **378**, 52 (1992), doi:10.1016/0550-3213(92)90003-T.
- 187 [10] H. Eguchi, Y. Koike and K. Tanaka, *Twist-3 Formalism for Single Transverse Spin*
188 *Asymmetry Reexamined: Semi-Inclusive Deep Inelastic Scattering*, Nucl. Phys. B
189 **763**, 198 (2007), doi:10.1016/j.nuclphysb.2006.11.016.
- 190 [11] K. Kanazawa, Y. Koike, A. Metz and D. Pitonyak, *Towards an explana-*
191 *tion of transverse single-spin asymmetries in proton-proton collisions: the role*
192 *of fragmentation in collinear factorization*, Phys. Rev. D **89**, 111501 (2014),
193 doi:10.1103/PhysRevD.89.111501.
- 194 [12] S. Heppelmann *et al.* (STAR Collaobration), *Large p_T Forward Transverse Single*
195 *Spin Asymmetries of π^0 Mesons at $\sqrt{s} = 200$ and 500 GeV from STAR*, Proc. Sci.,
196 DIS2013 (2013) 240, doi:https://doi.org/10.22323/1.191.0240.
- 197 [13] M. M. Mondal *et al.*, (STAR Collaboration), *Measurement of the Transverse Single-*
198 *Spin Asymmetries for π^0 and Jet-like Events at Forward Rapidities at STAR in p + p*
199 *Collisions at $\sqrt{s} = 510$ GeV*, Proc. Sci., DIS2014 (2014) 216, doi:10.22323/1.203.0216.

- 200 [14] J. Adam *et al.* (STAR Collaboration), *Measurement of transverse single-spin*
201 *asymmetries of π^0 and electromagnetic jets at forward rapidity in 200 and 500*
202 *GeV transversely polarized proton-proton collisions*, Phys. Rev. D **103**, 092009,
203 doi:10.1103/PhysRevD.103.092009.
- 204 [15] O. Adriani *et al.* (LHCf Collaboration), *Measurements of longitudinal and trans-*
205 *verse momentum distributions for neutral pions in the forward-rapidity region with*
206 *the LHCf detector* Phys. Rev. D **94**, 032007 (2016), doi:10.1103/PhysRevD.94.032007.
- 207 [16] C. Adler *et al.*, *The RHIC zero degree calorimeters* Nucl. Instru. Meth. A **470**, 488
208 (2001), doi:10.1016/S0168-9002(01)00627-1.
- 209 [17] C. A. Whitten Jr. *et al.* (STAR Collaboration), *The Beam-Beam Counter: A Local*
210 *Polarimeter at STAR*, <https://www.star.bnl.gov/~eca/LocalPol>.
- 211 [18] W. J. Llope *et al.*, *The STAR Vertex Position Detector*, Nucl. Instrum. Methods
212 Phys. Res., Sect. A **759**, 23 (2014), doi:10.1016/j.nima.2014.04.080.
- 213 [19] ALICE Collaboration, *Letter of Intent: A Forward Calorimeter (FoCal) in the ALICE*
214 *experiment*, CERN-LHCC-2020-009, <https://cds.cern.ch/record/2719928>.